Critical behavior in a polymer blend

H. Sato, N. Kuwahara, and K. Kubota
Department of Biological and Chemical Engineering, Faculty of Technology, Gunma University, Kiryu, Gunma 376, Japan
(Received 5 September 1995)

Static and dynamic critical behaviors were studied for a mixture of polydimethylsiloxane ($M_w = 1.91 \times 10^4$, $M_w/M_n < 1.03$) and polyethylmethylsiloxane ($M_w = 1.40 \times 10^4$, $M_w/M_n < 1.02$) using coexistence curve, turbidity, light scattering, and viscosity measurements. The critical point was determined precisely from the coexistence curve as the critical composition $W_{c,\mathrm{PEMS}} = 55.04$ wt % and the critical mixing temperature $T_c = 30.622$ °C. The critical exponents for the shape of the coexistence curve (β), the osmotic compressibility (γ), the long-range correlation length (ν), the correction for the static correlation function (η), and the shear viscosity (ϕ) are 0.327 ± 0.003, 1.25 ± 0.02, 0.63 ± 0.02, 0.038 ± 0.003, and 0.029 ± 0.003, respectively, with $\xi_0 = 1.62 \pm 0.05$ nm. The present critical polymer blend belongs to the universality class of the three-dimensional Ising model, similar to simple binary liquid mixtures. The crossover from Ising to mean-field behavior was not observed, and this observation is consistent with the crossover function of recent theoretical work. A clear shear effect on the viscosity was observed near the critical point. The critical part of the diffusion coefficient is rather well represented by the dynamic scaling function based on mode coupling theory, confirming the validity of the dynamic scaling concept for the polymer blend.

PACS number(s): 64.70.−p, 61.41.+e, 64.60.Fr

I. INTRODUCTION

Numerous experiments on the critical behaviors in polymer-polymer mixtures have been performed, and the validity of the three-dimensional Ising-model universality has been confirmed in the vicinity of the critical point by use of small-angle neutron scattering (SANS) [1,2], light scattering LS [3,4], and the phase diagram [5,6]. However, most of the experiments have been carried out without the accurate determination of the critical mixing point. For example, Meier, Momper, and Fisher have studied the critical behaviors for a mixture of polydimethylsiloxane (PDMS) and polyethylmethylsiloxane (PEMS) [3]. They have estimated a critical composition by the expectation $\phi_{c,\mathrm{PEMS}} = N_{\mathrm{PDMS}}^{1/2}/(N_{\mathrm{PEMS}}^{1/2} + N_{\mathrm{PDMS}}^{1/2})$ with N being the degree of polymerization of the respective polymer. By use of the critical point established by the concentration dependence of the spinodal temperature, we have investigated the critical behavior in a mixture of polystyrene and polymethylphenyisiloxane over the range $0.045 < T - T_c < 2.4$, ° C, where T_c is the critical mixing temperature [4]. The exponents for the osmotic compressibility χ_T and the long-range correlation length ξ are in good agreement with the three-dimensional Ising model universality, similarly to binary simple liquid mixing [7]. The crossover behavior from Ising to mean-field behavior was suggested for polymer blends by de Gennes. The characteristic crossover temperature, the Ginzburg number G_i, is also calculated from the relation $G_i \propto N^{-1}$ [8]. Therefore, the critical region is expected to be very narrow and the mean-field formalism becomes valid even near the critical point, quite different from the case of simple binary liquid mixtures. Although a polymer blend is expected to obey Ising-like behavior in the immediate neighborhood of the critical mixing point, an exact study concerning the critical behaviors in a polymer blend with accurate phase diagram and/or coexistence curve is still necessary. In the case of polymer blends, the cloud point curve often deviates from the coexistence curve, and the critical point is not located at the top of the cloud point curve because of its remaining polydispersity. Hence, it is necessary to check the criticality by the direct determination of the coexistence curve. In previous work, we have determined the critical mixing point from the accurate measurement of the coexistence curve for a polymer blend [9]. Consequently, it is possible to approach very closely to the critical point and to observe the limiting anomalous behavior of various quantities. This is of essential importance for detailed studies of critical phenomena in a polymer blend.

In this paper we report experimental studies of the critical behaviors for a mixture of PDMS and PEMS. The criticality was ascertained clearly on the basis of the coexistence curve [9]. The dynamical critical behaviors of the transport coefficients, the viscosity and diffusion coefficients, as well as of the static quantities, osmotic compressibility and long-range correlation length, were measured directly and analyzed with the aid of the recent theoretical work on the shear rate effect for fluctuation [10,11]. The critical PDMS-PEMS mixture was found to belong to the same universality class as the three-dimensional Ising model.

II. GENERAL FORMULATION

Here we summarize briefly the general formulation of the critical behaviors relevant to the present work.

A. Coexistence curve

Near the critical mixing point, the coexistence curve is well expressed by the scaling form

 ©1996 The American Physical Society

$$W^+ - W^- = B\varepsilon^\beta , \tag{1}$$

where W^+ and W^- are the concentrations of PEMS in coexisting concentrated and dilute phases, respectively. β is the critical exponent for the coexistence curve and ε is the reduced temperature defined as $\varepsilon = |T - T_c|/T_c$.

B. Static structure function

According to the theory of critical phenomena the static structure (correlation) function $S(q)$, which is proportional to the susceptibility and/or the scattered light intensity $I(q)$, can be expressed in a scaling form as [12]

$$S(q) = S(q=0)g(q\xi) = A_1 \chi_T g(q\xi) , \tag{2}$$

where A_1 is treated as a constant parameter insensitive to the temperature and q is the scattering vector. $g(q\xi)$ corresponds to the Fourier transform of the correlation function and is expressed in the Ornstein-Zernike form as

$$g(q\xi)^{-1} = (1 + q^2\xi^2) . \tag{3}$$

χ_T is the isothermal osmotic compressibility and ξ is the correlation length. Both diverge near the critical point as

$$\chi_T = \chi_{T,0}\varepsilon^{-\gamma} , \tag{4}$$

$$\xi = \xi_0 \varepsilon^{-\nu} , \tag{5}$$

with γ and ν being the critical exponents of χ_T and ξ, respectively. Fisher proposed a modified Ornstein-Zernike correlation function of the form $g(q\xi)^{-1} = (1 + q^2\xi^2)^{1-\eta/2}$ [13]. η is a small correction factor and it can be examined from the ξ dependence of χ_T (that is, ξ^2/χ_T vs ξ) using the hyperscaling relation

$$\gamma = (2 - \eta)\nu . \tag{6}$$

C. Turbidity

The turbidity τ is defined as the attenuation of transmitted light intensity per unit optical path length, and it results from the scattering when the sample does not absorb the incident beam. Using the Ornstein-Zernike form for the scattering function as in Eq. (3), the turbidity can be written as [14]

$$\tau = A_2 \chi_T G(z) , \tag{7}$$

where A_2 can be treated as a constant insensitive to temperature and

$$G(z) = [(2z^2 + 2z + 1)/z^3]\ln(1 + 2z) - 2(1 + z)/z^2 , \tag{8}$$

$$z = 2(q_0\xi)^2 , \tag{9}$$

where $q_0 (= 2\pi/\lambda_0)$ is the magnitude of the incident wave vector with λ_0 being the wavelength of the incident beam.

D. Dynamic structure function and transport coefficient

Light scattering detects composition fluctuation, which is the order parameter of the critical mixture sample. Its time correlation function can be represented by an exponential decay law of the form

$$\langle C_q(t) C_{-q}(0) \rangle = S(q)\exp(-\Gamma_q t) = S(q)\exp[-D(q)q^2 t] , \tag{10}$$

where $S(q)$ $[= \langle |C_q(0)|^2 \rangle]$ is the static correlation function with correlation length ξ given by Eq. (2) and $D(q)$ is the q-dependent diffusion coefficient obtained from the decay rate Γ_q of the time correlation function. The diffusion coefficient $D(q)$ is related to the Onsager kinetic coefficient L by [15]

$$D(q) = L/S(q) . \tag{11}$$

In the treatment of dynamic critical phenomena, the transport coefficients, such as the Onsager kinetic coefficient L and the shear viscosity η, can be separated into two terms [16,17]. One is the background contribution, L_B and η_B, and the other is the critical or singular contribution, L_c and η_c, so that

$$L = L_c + L_B , \tag{12}$$

$$\eta = \eta_c + \eta_B . \tag{13}$$

Here, L_c and η_c represent the transport coefficients due to the critical fluctuation, while L_B and η_B represent them without the critical fluctuation. Then, the diffusion coefficient also can be separated into two terms with the assumption that the background (noncritical) contribution of $S(q)$ to the measured $S(q)$ is negligible, which is valid enough in the critical region, as

$$D = D_c + D_B = L_c/S(q) + L_B/S(q) . \tag{14}$$

The asymptotic equations of the diffusion coefficient and the shear viscosity satisfy the following equations according to the theories [18]:

$$D_c = (k_B T/6\pi\eta\xi)\Omega(q\xi) , \tag{15}$$

$$\eta = \eta_B (Q_0\xi)^z = \eta_B (Q_0\xi_0)^z \varepsilon^{-\phi} , \tag{16}$$

where the dynamic scaling function $\Omega(q\xi)$ is represented by the Kawasaki function following from the mode coupling theory [19] as

$$\Omega(x) = \Omega_K(x) \equiv (3/4x^2)[1 + x^2 + (x^3 - 1/x)\arctan x] . \tag{17}$$

On the other hand, Burstyn *et al.* introduced the correction factor $S(x)$ including a viscosity correction into the dynamic scaling function for the deficiency of the Kawasaki function at large scaling variable $q\xi$ [20,21]:

$$\Omega(x) = \Omega_K(x)[S(x)]^z , \tag{18}$$

$$S(x) = a(1 + b^2x^2)^{1/2} , \tag{19}$$

where a and b are constants and are approximated to $a^z = R = 1.01$, with R being the dynamic amplitude ratio, and $b = 0.5$ [20]. Moreover, the background contribution D_B can be approximated as [22,23]

$$D_B = (k_B T/16\eta_B\xi)(1 + q^2\xi^2)/q_c\xi , \tag{20}$$

where q_c is a parameter related to Q_0 and q_D, the Debye cutoff wave number, and is obtained from [24]

$$Q_0^{-1}=\tfrac{1}{2}e^{4/3}(q_c^{-1}+q_D^{-1}) . \quad (21)$$

Thus the dynamical scaling behavior can be examined by using the reduced diffusion coefficient D^* defined as

$$D^*=(6\pi\eta\xi/k_BT)D_c . \quad (22)$$

On the other hand, η_B is represented by the well known Arrhenius equation of the form

$$\eta_B=A_\eta\exp(B_\eta/T) , \quad (23)$$

and z is predicted to be 0.054 by the mode coupling theory [25]. ϕ is given by

$$\phi=\zeta\nu . \quad (24)$$

E. Shear effect

The shear rate effect on the critical phenomena has been discussed by Onuki and Kawasaki [10]. A shear applied to the measured test sample makes the fluctuations anisotropic and destroys the correlations eventually. This crossover will occur when the lifetime τ_L of the fluctuation becomes comparable to the intrinsic time of shear, the inverse of the shear rate S, and the crossover temperature T_s is given by

$$T_s=T_c[1+(16\eta\xi_0^3/k_BT_c)^{1/3\nu}S^{1/3\nu}] . \quad (25)$$

In the eventual strong shear region, $S\tau_L>1$, the critical fluctuation should show a mean-field behavior. In the presence of shear the critical temperature is also expected to be affected by the reduction of fluctuation and the critical temperature under the shear, T_c^*, is predicted to be

$$T_c^*=T_c-v(T_s-T_c) , \quad (26)$$

where v is a numerical constant and is predicted to be $\frac{1}{12}$ [10,11,26]. Therefore, the critical behavior of the shear viscosity must be taken into account in this shear rate effect.

III. EXPERIMENT

Polydimethylsiloxane having kinematic viscosity of 300 cS obtained from Shin-Etsu Co. was fractionated into seven fractions by solution fractionation using isopropyl alcohol as the solvent. A fraction characterized as $M_w=1.91\times10^4$ and $M_w/M_n<1.03$, with M_w and M_n being the weight- and number-averaged molecular weights, respectively, was used in this study. Polyethylmethylsiloxane specially synthesized by Shin-Etsu Co. was fractionated into 11 fractions by solution fractionation using n-propyl formate as the solvent. A fraction characterized as $M_w=1.40\times10^4$ and $M_w/M_n<1.02$ was employed as the sample. Our polymer samples are almost free from the polydispersity effect. The values of density and refractive index of PDMS and PEMS at 25° C are 0.969 and 0.977 g/cm^3, and 1.403 and 1.427, respectively. Both the density and refractive index of PDMS and PEMS are matched well. Thus our mixture sample greatly reduces the effects of multiple scattering and sedimentation.

The detailed experimental procedure for the measurements of coexistence curve and turbidity has been described elsewhere [9,27]. The mixture of 55.05 wt % PEMS in PDMS, which was determined to be the critical composition from the phase diagram, was prepared in a dry box under dry nitrogen for the measurements of the static and dynamic scattering and the shear viscosity. Particular attention was paid to avoiding moisture in the air. The homogeneous mixture, heat treated at 50° C and well stirred, was filtered into a cylindrical cell of 14 mm optical path length and a specially designed Ubbelohde-type viscometer through a Millipore filter (pore size = 0.20 μm), and then the polymer samples in the cylindrical cell and in the viscometer were flame sealed under vacuum. Those mixtures were thoroughly stirred with a piece of magnetic material which was inserted in the cell and in the viscometer. The cell for the light scattering measurement was set in a thermostattred silicon oil bath whose temperature could be controlled to within 1 mK over a day, and the viscometer was set in a thermostatted water bath regulated within 1 mK over two days in the experimental temperature range. The temperature was monitored by a quartz thermometer.

The angular dependence of the scattered light intensity was measured using a specially designed light scattering photometer with a He-Ne laser operated at 632.8 nm as a light source. The alignment of the photometer was checked by using a cyclohexane solution of low molecular weight polystyrene ($M_w=1.02\times10^4$). The observed scattered light intensity after scattering volume correction was found to be constant within 1% over an angular range of $\theta=20°-130°$. Intensity measurements were carried out in the temperature range $0.020\le T-T_c\le5.413$° C. The scattered light intensity at a temperature about 15° C away from T_c was used as the background intensity and was subtracted from the measured scattered light intensity. The intensity was corrected for attenuation using turbidity data. Since the turbidity of our sample is low enough, no multiple-scattering correction was undertaken. The dynamic light scattering measurement (time correlation function measurement) was performed at $\theta=60°$, 90°, and 130° in the temperature range $0.020\le T-T_c\le9.436$° C. The intensity-intensity time correlation functions were measured with a 48-channel Malvern correlator. Viscosity measurements were performed in the temperature range $0.010\le T-T_c\le11.208$° C using the modified Ubbelohde viscometer which was calibrated by comparing the flow time of n-amyl alcohol (flow time is about 101 s) with density correction. The shear rate was calculated using a Poiseuille law for capillary flow assuming Newtonian flow [28], and the averaged shear rate at the closest temperature to T_c was about 2 s^{-1}.

IV. RESULTS AND DISCUSSION

A. Phase diagram

The coexistence curve near the critical mixing point is shown in Fig. 1 together with the diameter. An accurate coexistence curve for the polymer-polymer mixture was

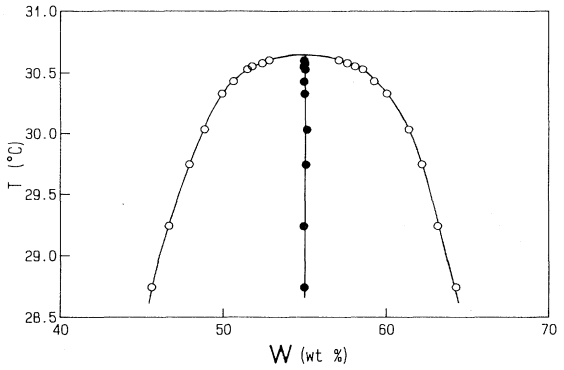

FIG. 1. Coexistence curve (○) and diameter (●) of a polymer blend of PDMS and PEMS. The critical point was determined from their intersection; $W_{c,\mathrm{PEMS}}=55.04\pm0.04$ wt % and $T_c=30.622\pm0.005$ °C.

obtained, although a thorough attainment of phase equilibrium between two coexisting phases needs three weeks near the critical point. The coexistence curve is almost symmetric, the diameter is almost perpendicular, and a deviation from the rectilinear was not observed. From the intersection of the coexistence curve with the diameter, the critical concentration and temperature were determined as $W_{c,\mathrm{PEMS}}=55.04\pm0.04$ wt % and $T_c=30.622\pm0.005$° C. The critical concentration expected from mean-field theory is 56.2 wt %, showing a little deviation from the exact one. Figure 2 shows the double-logarithmic plot of the concentration difference between the concentrated and dilute phases as a function of T_c-T. The simple scaling form of Eq. (1) describing the coexistence curve holds very well, and the linear fit to Eq. (1) for the data at $T-T_c<2$° C gives $\beta=0.327\pm0.003$ with $B=97.9\pm3.0$ wt %. The residuals are quite small and do not show any systematic deviation (variance $<1\%$). The exponent β is in very good agreement with

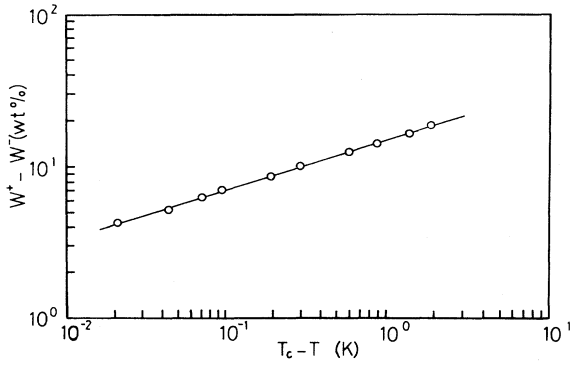

FIG. 2. Double-logarithmic plot of the concentration difference between two coexisting phases of a PDMS and PEMS mixture as a function of T_c-T. W^+ and W^- denote the concentration of PEMS in the concentrated and dilute phases, respectively. The slope of the solid line is 0.327 ± 0.003.

the experimental values for simple binary liquid mixtures and the three-dimensional Ising model [29–31]. This β value differs clearly from the mean-field prediction of 0.5, and the concentration difference in Fig. 2 does not show a crossover between Ising and mean-field behavior in the present temperature range. Coexistence curves for binary polymer mixture have been reported by Chu *et al.* [5] and Budkowski *et al.* [6]. Both have reported that the coexisting phase equilibrium behavior is well expressed by mean-field theory. However, both measurements were carried out fairly far away from the critical point, because of the experimental difficulty due to the high shear viscosity of the sample polymers. According to the theoretical treatment of crossover behavior [32–34], the crossover from mean-field to Ising behavior should take place closer to the critical point with increasing molecular weight. Thus it is essential to come very close to the critical point for studying the critical behavior. In the present case, it is expected that the crossover may take place at about a few ° C away from T_c from an evaluation based on the results of Meier *et al.* [34], and that the three-dimensional Ising behavior can be observed.

B. Static structure function

Typical results of static light scattering measurements are shown in Fig. 3. The scattered light intensity at a temperature about 15° C away from T_c was used as the

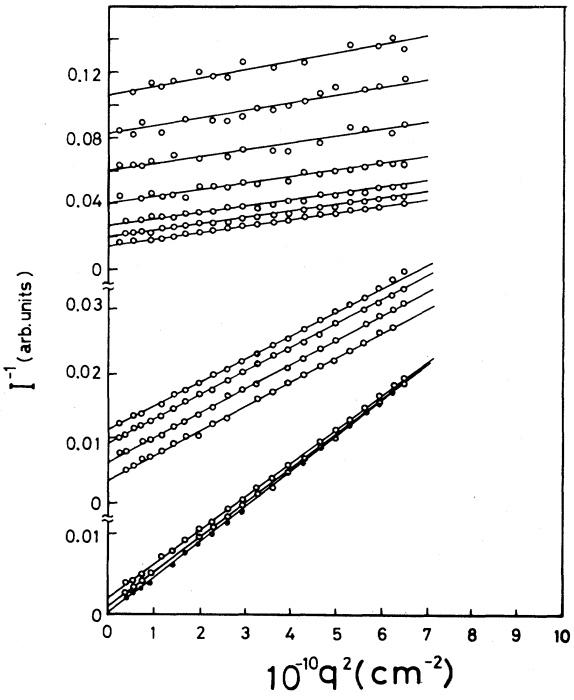

FIG. 3. Ornstein-Zernike plot of the scattered light intensity as a function of q^2 at a few typical temperatures. Attenuation due to turbidity was corrected for. The temperature of the curve is 35.997, 35.002, 34.015, 33.229, 32.594, 32.189, 31.890, 31.681, 31.516, 31.130, 30.968, 30.846, 30.752, and 30.656 °C from the top to the bottom, respectively.

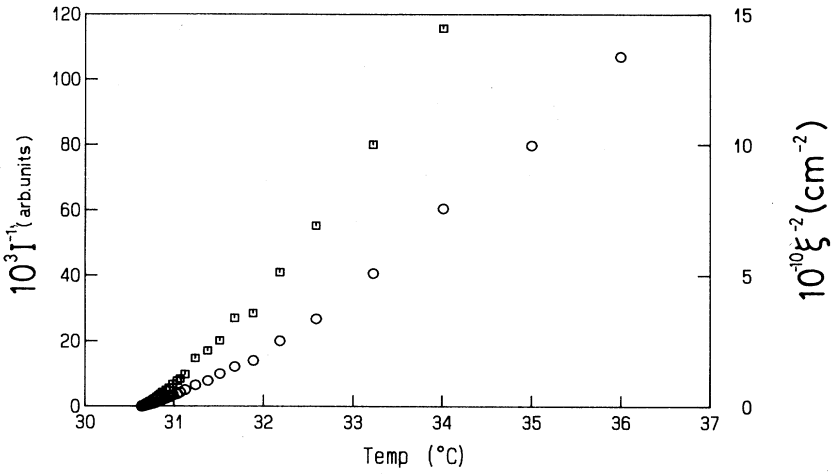

FIG. 4. Temperature dependence of I_0^{-1} and ξ^{-2}. The temperature extrapolated to I_0^{-1} and $\xi^{-2}=0$ is 30.622 °C. The symbols ○ and □ denote I_0^{-1} and ξ^{-2}, respectively.

background intensity and was subtracted from the measured scattered light intensity at the experimental temperature in order to avoid the possible contributions of particle scattering of the polymer molecules. The present evaluation of the background intensity is not a unique one; other methods are possible. Indeed, Meier *et al.* used the intensity estimated from the volume fraction. If we are interested in the critical behavior very near the critical point, however, the method used does not make any essential difference. As shown in Fig. 3, the Ornstein-Zernike plot of Eqs. (2) and (3) gives reasonably good straight lines, suggesting the validity of the static correlation function of Eq. (3). Although no downward curvatures at small scattering angles were observed near T_c, slight deviations from parallel slopes at temperatures closer to T_c are observed, indicating nonzero η in Eq. (6) [35–37].

The inverse of the zero-angle scattered light intensity I_0^{-1} and the squared inverse of the correlation length ξ^{-2} obtained through Eq. (3) are shown in Fig. 4 as a function of temperature. Both curves show no linear dependence on the temperature, rejecting the mean-field behavior especially near T_c. The temperatures extrapolated to $I_0^{-1}=0$ and $\xi^{-2}=0$ coincide perfectly with each other and with the result of the coexistence curve. These facts indicate firmly the criticality of the critical point determined above.

Double-logarithmic plots of I_0^{-1} and ξ as a function of the reduced temperature are shown in Fig. 5. Both are well represented by the power-law relations of Eqs. (4) and (5) in almost the total experimental temperature range, and $\gamma=1.25\pm0.02$, $\nu=0.63\pm0.02$, together with $\xi_0=1.62\pm0.05$ nm were obtained. These values of the critical exponents are in quite good agreement with the three-dimensional Ising model. The magnitude of ξ_0 is comparable with the reported value of 1.67 nm for PDMS-PEMS [34], 1.0 nm for polystyrene-polymethylphenylsiloxane (PS-PMPS) [4], and 0.70 nm for deutero-polybutadiene-polystyrene (*d*-PB-PS) [37].

The crossover from Ising to mean-field behavior in polymer blends has been studied intensively by Meier *et al.* and Schwahn *et al.*, and it has been shown that the crossover behavior is well expressed by the crossover function given in Eq. (27) of the asymptotic crossover model by introducing a Ginzburg number G_i [32–34]. The crossover function as derived by Belyakov and Kiselev [33] is given by

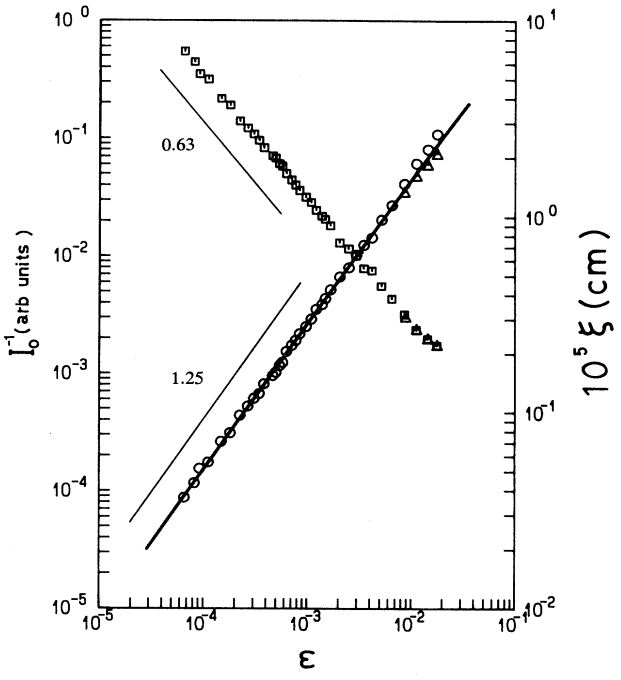

FIG. 5. Double-logarithmic plots of I_0^{-1} and ξ as a function of the reduced temperature. The symbols ○ and □ denote I_0^{-1} and ξ with subtraction of the background intensity, respectively, and the symbol △ denotes them without subtracting it. The slopes of the respective data points near the critical point give $\gamma=1.25\pm0.02$ and $\nu=0.63\pm0.02$ with $\xi_0=1.62\pm0.05$ nm. A clear crossover from Ising to mean-field behavior is not observed in the experimental temperature range. The solid curve is the susceptibility calculated from the crossover function with $G_i=2\times10^{-2}$ fitted to the experimental data.

$$\hat{\tau}=[1+2.333\hat{S}(0)^{\Delta/\gamma}]^{(\gamma-1)/\Delta}\{\hat{S}(0)^{-1}+[1+2.333\hat{S}(0)^{\Delta/\gamma-\gamma/\Delta}\}\ , \quad (27)$$

where $\hat{\tau}=\tau/G_i$ with $\tau=|T_c^{-1}-T^{-1}|/T_c^{-1}$ and $\hat{S}(0)=S(0)G_i/C_{\rm MF}$. $C_{\rm MF}$ is a characteristic parameter, being the critical amplitude of the susceptibility of the mean-field approximation. Δ is the universal correction to the scaling exponent and is 0.5. The results for I_0^{-1} and ξ obtained without subtracting the background intensity are also plotted in Fig. 5 in order to examine the crossover behavior. The difference between the subtracted and the unsubtracted data is negligibly small except for a few data points far away from the critical point. Since the scattered light intensity is not calibrated to give the absolute static structure function in our case, we could not obtain the parameter $C_{\rm MF}$ in the crossover function. However, we can evaluate G_i roughly as about 2×10^{-2} in a good approximation from the overall characteristics of the crossover function and in reasonable agreement with the results of Meier *et al.* [34], although a small deviation for the two data points farthest from the critical point is observed. Schwahn *et al.* have pointed out that the mean-field approximation becomes valid enough above $\varepsilon=300G_i$ and the critical composition fluctuations are still strong enough even at 15°C away from T_c [38]. Therefore the procedure for extracting the critical part of the susceptibility by subtracting the scattered intensity at 15°C away from T_c is not exact enough. However, the essential critical behavior is the same for both the subtracted and unsubtracted methods, as is shown in Fig. 5. The G_i value is considerably larger than the prediction of de Gennes, $G_i \propto N^{-1}$ with N being the degree of polymerization [8]. The breakdown of N^{-1} scaling of G_i could be related to the fact that sufficient entanglements between polymer chains are not formed in the present system. Unexpectedly large values of G_i have been observed and discussed by Schwahn *et al.* in relation to the nonuniversality of G_i and the free volume effect [38–40]. This wide critical region for polymer blend systems may result in the rather easy experimental ascertainment of the three-dimensional Ising model universality and of the breakdown of the mean-field approximation for polymer blends, even without approaching the immediate neighborhood of the critical point and the accurate determination of the critical point.

Figure 6 shows the double-logarithmic plot of ξ^2/I_0 vs ξ. Since ξ^2/I_0 is in proportion to $\varepsilon^{\gamma-2\nu}=(\varepsilon^{-\nu})^{(2\nu-\gamma)/\nu}=(\varepsilon^{-\nu})^{\eta}$ near the critical point, the slope of this plot gives the exponent η. The linearity of the data is good, indicating the validity of the hyperscaling relation, and $\eta=0.038\pm0.003$ was obtained. This value is in very good agreement with the results for binary liquid mixtures and the three-dimensional Ising model. Janssen, Schwahn, and Springer obtained $\eta=0.047$ for *d*-PB-PS by SANS [37]. Schwahn, Mortensen, and Janssen investigated η in both the stable and unstable regions. The η value of 0.038 obtained in the stable region is in good agreement with the renormalization-group prediction, but a negative η value was observed in the unstable region [41].

C. Turbidity

Since the Ornstein-Zernike form for the correlation function is valid for the present system, the turbidity should be represented by Eq. (7). Figure 7 shows the double-logarithmic plot of the turbidity as a function of the reduced temperature. Since the difference between the refractive index of the respective polymers is small, the turbidity is relatively low ($\tau\sim0.2$ at $\varepsilon\sim10^{-4}$). The exponent γ and ν were determined by a nonlinear least squares fit to Eq. (7). The fitting was good, as shown in the inset deviations in Fig. 7, and $\gamma=1.20\pm0.06$ and $\nu=0.65\pm0.03$ were obtained together with $\xi_0=1.37\pm0.35$ nm. These values are in reasonable agreement with the exponent values of the static light scattering experiment because of the monotonic nature of turbidity.

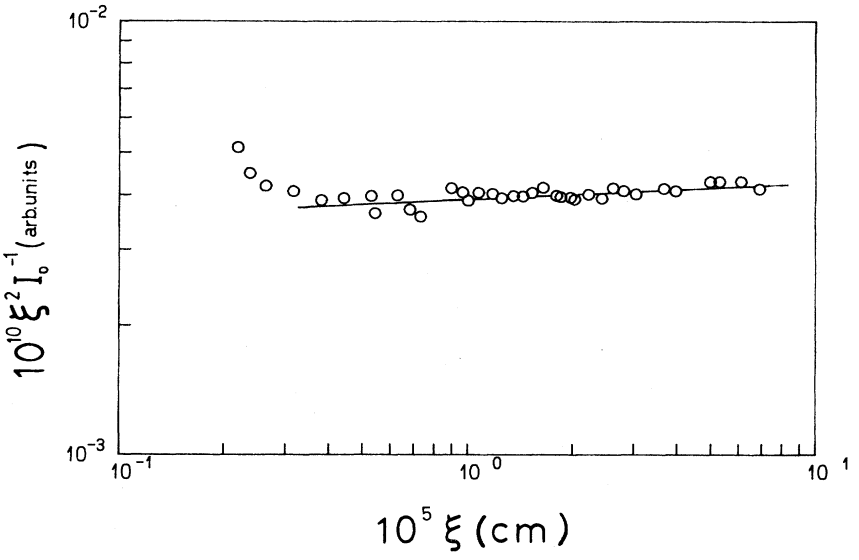

FIG. 6. Double-logarithmic plot of ξ^2/I_0 vs ξ. The straight line has a slope of 0.038 ± 0.003, which corresponds to the exponent η.

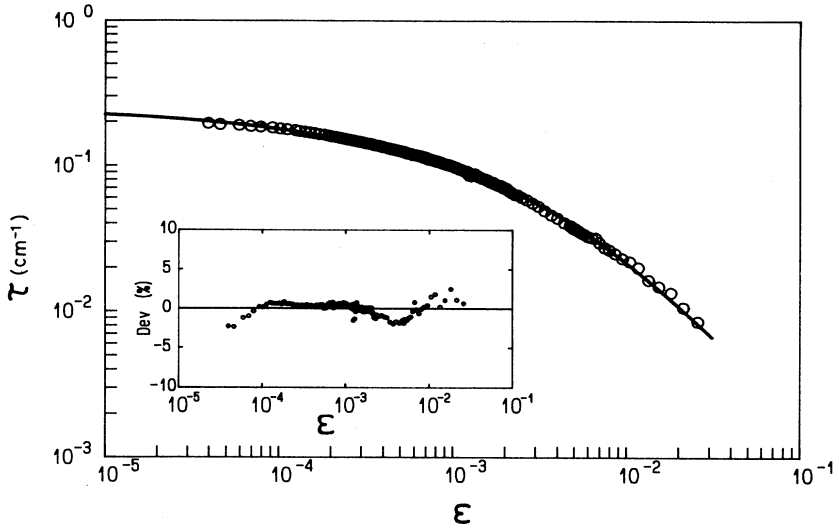

FIG. 7. Double-logarithmic plot of turbidity as a function of the reduced temperature ε. The solid curve is the one fitted by Eq. (7) with $\nu=0.65\pm0.03$, $\gamma=1.20\pm0.06$, and $\xi_0=1.37\pm0.35$ nm.

D. Shear viscosity

The result for the shear viscosity measured directly using the modified Ubbelohde viscometer is shown in Fig. 8. The flow time close to T_c became about 10^4 s and the magnitude of the shear viscosity was about 4 P. Since a weak critical anomaly in the shear viscosity appears near the critical point, the background viscosity η_B was evaluated using five points in the range $10^3/T=3.175-3.247$. The resultant background shear viscosity $\ln\eta_B$ is expressed well by the Arrhenius equation $\eta_B=-6.168+2.285\times10^3/\mathrm{T}$.

η/η_B is plotted double logarithmically as a function of the reduced temperature in Fig. 9. The data points show a clear deviation from the linearity very near T_c. The shear rate at the closest temperature to T_c is very low and is evaluated to be about 2 s^{-1}. Because the magnitude of η is very large ($\sim$4 P), the shear effect to the critical fluctuation becomes non-negligible. According to the theory of Onuki and co-workers [10,26], the crossover from weak shear to strong shear may take place at around T_s defined by Eq. (25). The value of T_s-T_c is predicted to be 0.77 K. This temperature is located near where η/η_B starts to show a deviation from linearity, and the reduction of critical fluctuation due to a finite shear rate is detected clearly. Therefore the shift of the critical temperature should be taken into account, and it was evaluated to be 64 mK according to Eq. (26). Figure 9 was drawn considering this shift of the critical temperature.

The evaluation of the exponent ϕ was carried out using the data points in the middle portion of the figure, where the linearity is good, and $\phi=0.029\pm0.03$ was obtained. Similarly Q_0 in Eq. (16) was obtained as 3.91×10^5 cm^{-1} or $Q_0^{-1}=25.6$ nm. The exponent z was obtained as 0.046 ± 0.007 from the relation of Eq. (24) using $\nu=0.63$. The value 0.054 for the exponent z is predicted from mode coupling theory and is in reasonable agreement with the above experimental result [25].

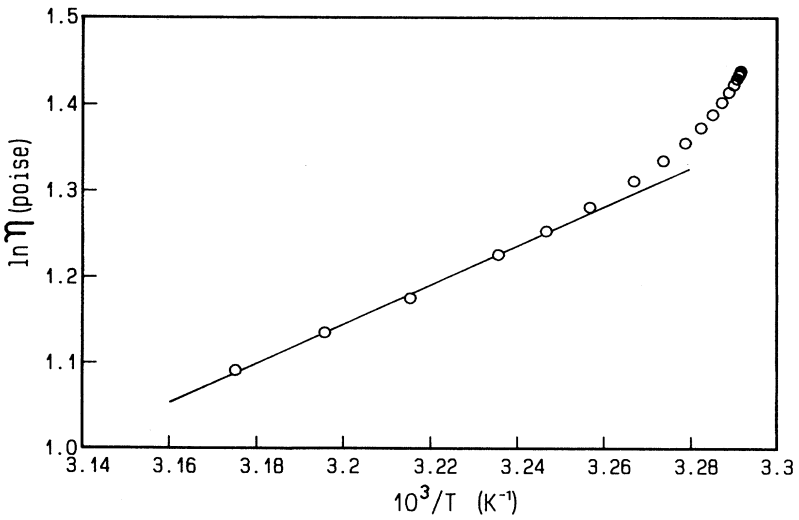

FIG. 8.. Shear viscosity of critical PDMS-PEMS mixture as a function of the inverse temperature. The straight line denotes the background viscosity.

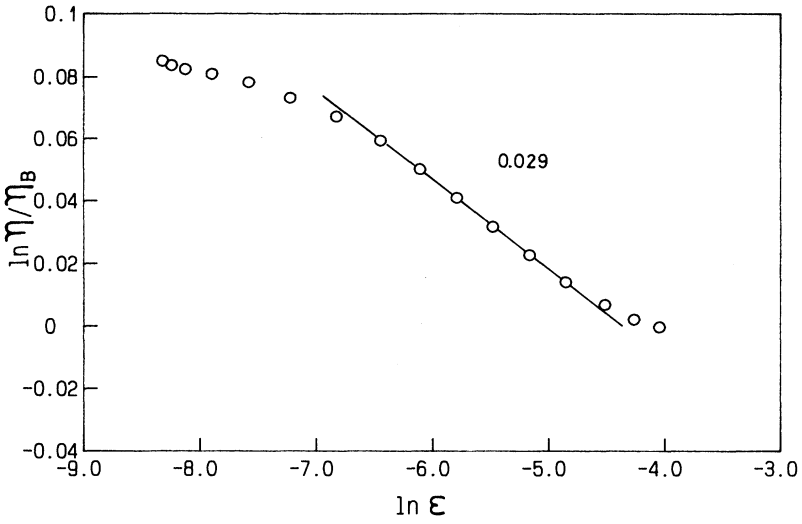

FIG. 9. $\ln\eta/\eta_B$ vs $\ln\varepsilon$. The straight line has a slope $-0.029(\phi=0.029\pm0.003)$. In the left side of the figure η/η_B shows a deviation from a straight line, indicating the reduction of fluctuation due to a finite shear rate. The crossover temperature T_s is $T_c+0.77$ K.

E. Diffusion coefficient

The measured time correlation functions showed good single-exponential decay functions with time, and the decay rate or Rayleigh linewidth Γ_q at the scattering vector q was obtained from the fitting of the initial slope. The decay rate is shown in Fig. 10 as a function of ε. A temperature-independent Γ_q is obtained close to T_c as observed in the usual dynamic critical phenomena. Γ_q varies from q^2 dependence corresponding to the hydrodynamic region to nondiffusive q^3 dependence on approaching T_c. The diffusion coefficient is shown in Fig. 11; it is q dependent near T_c and becomes q independent far away from T_c.

The diffusion coefficient can be divided into two parts, the critical part and the background part, as in Eq. (14). In order to examine the dynamical critical behavior it is necessary to evaluate the background contribution. We selected the method of Burstyn *et al.* [20] of Eq. (20) for the background estimation. q_c is related to both Q_0 and q_D. Although Q_0 is obtained from the measurement of shear viscosity, we need to evaluate q_D. The procedure of Oxtoby and Gelbart [22] gives $q_D^{-1}=0$ and a too large q_c^{-1} as noted by Burstyn *et al.* [20]. Therefore we used the method of Burstyn *et al.* as $q_c=q_D$, and $q_c^{-1}=6.8$ nm was obtained. It should be noted that this procedure gives $q_D^{-1}=6.8$ nm too, and this value is quite comparable with the value of 7.5 nm of Meier, Momper, and Fisher [3].

Figure 12 shows the reduced diffusion coefficient as a function of the scaling variable $q\xi$. The $q\xi$ value reaches almost 20 and the critical nondiffusive region is realized. The solid line shows the Kawasaki function $\Omega_K(q\xi)$ for the dynamic scaling function where the shear viscosity is corrected for zero shear rate. The experimental data points at three different scattering angles do not collapse completely to form a single master curve and show a little systematic deviation from each other. This fact might re-

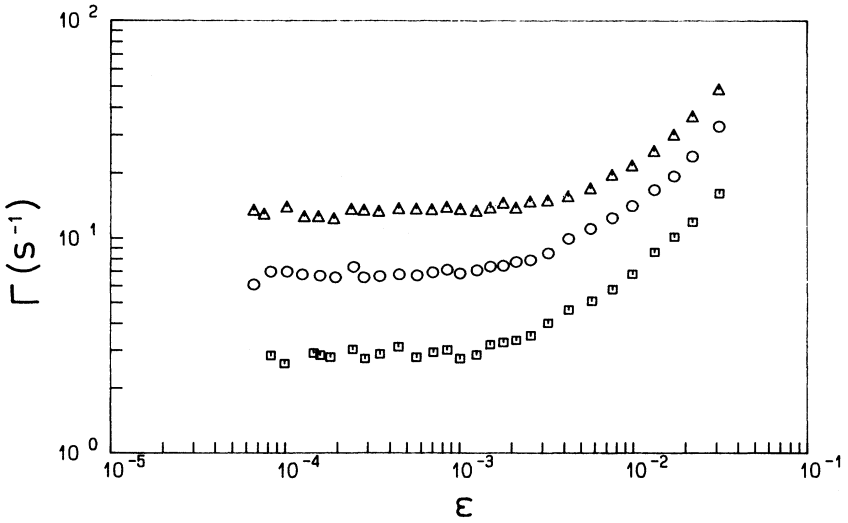

FIG. 10. Decay rate Γ_q as a function of the reduced temperature obtained from the dynamic light scattering at three scattering angles. □, ○, and △ denote $\theta=60°$, 90°, and 130°, respectively. Γ_q varies from a q^2 dependence to a q^3 dependence on approaching T_c.

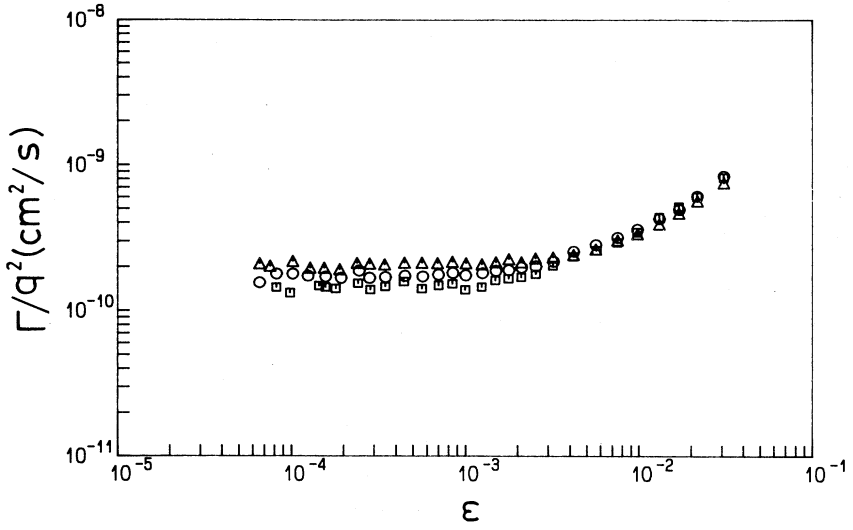

FIG. 11. Diffusion coefficient Γ/q^2 $(=D)$ as a function of the reduced temperature. The notation for the symbols is the same as in Fig. 10.

sult from the inaccuracy of the determination of q_c, or could mean that the time correlation function has a contribution from some other mode (for example, entanglement) than the mutual diffusional mode. At present the definite reason is not clear. However, the overall characteristics of the data points show a universal nature, confirming the validity of dynamical scaling for the order-parameter fluctuations and a deviation from $\Omega_K(q\xi)$ especially at large $q\xi$. The dotted curve is the corrected dynamic scaling function obtained from Eqs. (18) and (19) where R and b were set at 1.01 and 0.5, respectively. The agreement between the dotted curve and the experimental D^* is rather satisfying and shows the validity of the corrected dynamic scaling function especially for $\theta=90^\circ$.

V. CONCLUSION

In this paper we investigated static and dynamic critical behavior using a polymer-polymer mixture of well fractionated PDMS and PEMS with molecular weights of the order of 10^4. The essential points of the results are summarized as follows.

(1) A very precise coexistence curve was obtained and the critical exponent β is obtained as 0.327 ± 0.003 at a temperature close to the critical point for the polymer blend. The critical composition and temperature of the polymer blend are obtained accurately, and a very close approach to the critical mixing point was possible.

(2) Static structure function experiments gave the critical exponents $\gamma=1.25\pm0.02$, $\nu=0.63\pm0.02$, and $\eta=0.038\pm0.003$ with $\xi_0=1.62\pm0.05$ nm. A turbidity measurement gave reasonable agreement with the results of the static light scattering experiments. By the accurate determination of and the close approach to the critical point, it was firmly ascertained that the obtained critical exponents are in very good agreement with the three-dimensional Ising model. The polymer blend in the close neighborhood of the critical point belongs to the universality class of the three-dimensional Ising model, similar-

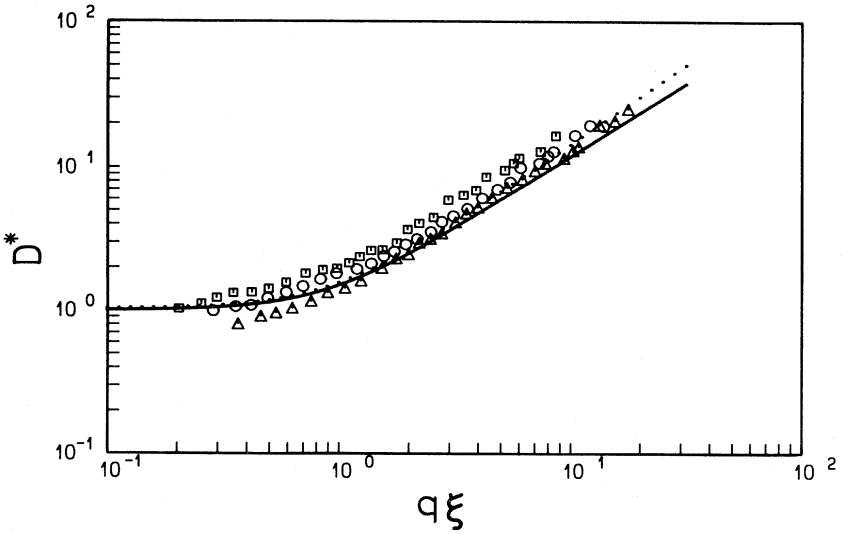

FIG. 12. Reduced diffusion coefficient D^* $(=6\pi\eta\xi D_c/k_BT)$ plotted double logarithmically as a function of the scaling variable $q\xi$. The notation for the symbols is the same as in Fig. 10. The solid curve represents the Kawasaki function $\Omega_K(q\xi)$ and the dotted curve represents the corrected dynamic scaling function proposed by Burstyn *et al.* [20] with $R=1.01$ and $b=0.5$, showing good agreement with the experimental D^*.

ly to simple binary liquid mixtures and polymer solutions.

(3) The crossover from Ising behavior to mean-field behavior was not observed clearly in the present experiment. The observation for the present polymer blend is consistent with the crossover function of recent theoretical work, indicating an unexpectedly wide critical region different from the prediction of de Gennes. A full understanding of the crossover behavior still needs further experimental study for a system having smaller G_i (larger molecular weight) over a wide temperature range.

(4) The shear viscosity of the critical polymer blend was directly measured and the reduction of the order-parameter fluctuation due to the finite shear rate was detected. The background viscosity is well expressed by an Arrhenius-type equation. The critical exponents $\phi=0.029\pm0.003$ and $z=0.046\pm0.007$ are in good agreement with the mode coupling theory.

(5) The diffusion coefficient shows the validity of the dynamical scaling and the dynamic scaling function is well expressed by the dynamic scaling function of corrected mode coupling theory. The background contribution to the diffusion coefficient for the polymer blend is properly evaluated, although further experimental study is still necessary for polymer blends.

ACKNOWLEDGMENTS

The authors with to thank T. Kawamata, K. Isojima, H. Yamoto, and M. Iguchi of Gunma University for their help in the measurement of the turbidity. This work was partly supported by the Ministry of Education, Science, Sports and Culture in Japan.

[1] D. Schwahn, K. Mortensen, T. Springer, H. Yee-Madeira, and R. Thomas, J. Chem. Phys. **87**, 6078 (1987); D. Schwahn, S. Janssen, and T. Springer, *ibid.* **94**, 8289 (1992).

[2] F. S. Bates, J. H. Rosedale, P. Stepanek, T. P. Lodge, P. Wiltzius, G. H. Frederickson, and R. P. Hjelm, Jr., Phys. Rev. Lett. **65**, 1893 (1990).

[3] G. Meier, B. Momper, and E. W. Fisher, J. Chem. Phys. **97**, 5884 (1992).

[4] N. Kuwahara, H. Sato, and K. Kubota, Phys. Rev. E **48**, 3176 (1993).

[5] B. Chu, K. Linliu, Q. Ying, T. Nose, and M. Okada, Phys. Rev. Lett. **68**, 3184 (1992).

[6] A. Budkowski, U. Steiner, J. Klein, and G. Schatz, Europhys. Lett. **18**, 705 (1992).

[7] H. E. Stanley, *Introduction to Phase Transitions and Critical Phenomena* (Oxford University Press, Oxford, 1971).

[8] P. G. de Gennes, *Scaling Concepts in Polymer Physics* (Cornell University Press, Ithaca, 1979).

[9] N. Kuwahara, H. Sato, and K. Kubota, Phys. Rev. Lett. **75**, 1534 (1995).

[10] A. Onuki and K. Kawasaki, Prog. Theor. Phys. Suppl. **64**, 436 (1978); Ann. Phys. (N.Y.) **121**, 456 (1979).

[11] D. Beysens, M. Gbadamassi, and B. Moncef-Bouanz, Phys. Rev. A **28**, 2491 (1983).

[12] M. E. Fisher, J. Math. Phys. **5**, 944 (1964).

[13] M. E. Fisher, Rept. Prog. Phys. **30**, 615 (1967).

[14] V. G. Puglielli and N. C. Ford, Phys. Rev. Lett. **25**, 143 (1973).

[15] L. van Hove, Phys. Rev. **95**, 1374 (1954).

[16] J. V. Sengers, in *Critical Phenomena,* Proceedings of the International School of Physics "Enrico Fermi," Course LI, edited by M. S. Green (Academic, New York, 1971).

[17] K. Kawasaki, in *Phase Transitions and Critical Phenomena,* edited by C. Domb and M. S. Green (Academic, New York, 1976), Vol. 5A.

[18] P. C. Hohenberg and B. I. Halperin, Rev. Mod. Phys. **49**, 435 (1977).

[19] K. Kawasaki, Ann. Phys. (N.Y.) **61**, 1 (1970).

[20] H. C. Burstyn, J. V. Sengers, J. K. Bhattacharjee, and R. A. Ferrell, Phys. Rev. A **28**, 1567 (1983).

[21] K. Kawasaki and S. Lo, Phys. Rev. Lett. **29**, 48 (1972).

[22] D. Oxtoby and W. Gelbart, J. Chem. Phys. **61**, 2957 (1973).

[23] J. K. Bhattacharjee, R. A. Ferrell, R. S. Basu, and J. V. Sengers, Phys. Rev. A **24**, 1469 (1981).

[24] R. Perl and R. A. Ferrell, Phys. Rev. Lett. **29**, 51 (1972); Phys. Rev. A **6**, 2358 (1972).

[25] T. Ohta, J. Phys. C **10**, 791 (1977).

[26] A. Onuki, K. Yamazaki, and K. Kawasaki, Ann. Phys. (N.Y.) **131**, 217 (1981).

[27] M. Nakata, N. Kuwahara, and M. Kaneko, J. Chem. Phys. **62**, 4278 (1975).

[28] L. D. Landau and E. M. Lifshitz, *Fluid Mechanics* (Pergamon, Oxford, 1959).

[29] D. Beysens, J. Chem. Phys. **71**, 2557 (1979).

[30] M. Nakata, T. Dobashi, N. Kuwahara, M. Kaneko, and B. Chu, Phys. Rev. A **18**, 2683 (1978).

[31] J. C. Le Guillou and J. Zinn-Justin, Phys. Rev. Lett. **39**, 95 (1977).

[32] M. A. Anisimov, S. B. Kiselev, J. V. Sengers, and S. Tang, Physica A **188**, 487 (1992).

[33] M. Y. Belyakov and S. B. Kiselev, Physica A **190**, 75 (1992).

[34] G. Meier, D. Schwahn, K. Mortensen, and S. Janssen, Europhys. Lett. **22**, 577 (1993).

[35] K. Kubota, N. Kuwahara, and H. Sato, J. Chem. Phys. **100**, 4543 (1994).

[36] Q. H. Lao, B. Chu, and N. Kuwahara, J. Chem. Phys. **62**, 2039 (1975).

[37] S. Janssen, D. Schwahn, and T. Springer, Phys. Rev. Lett. **68**, 3180 (1992).

[38] D. Schwahn, G. Meier, K. Mortensen, and S. Janssen, J. Phys. (France) II **4**, 837 (1994).

[39] D. Schwahn, H. Takeno, L. Willner, H. Hasegawa, H. Jinnai, T. Hashimoto, and M. Imai, Phys. Rev. Lett. **73**, 3427 (1994).

[40] D. Schwahn, T. Schmackers, and K. Mortensen, Phys. Rev. E **52**, R1288 (1995).

[41] D. Schwahn, K. Mortensen, and S. Janssen, Phys. Rev. Lett. **73**, 1452 (1994).